

# Spectrum for Nonmagnetic Mott Insulators from Power Functional within Reduced Density Matrix Functional Theory

Y. Shinohara,<sup>†</sup> S. Sharma,<sup>\*,†,‡</sup> S. Shallcross,<sup>¶</sup> N. N. Lathiotakis,<sup>†,§</sup> and E. K. U. Gross<sup>†</sup>

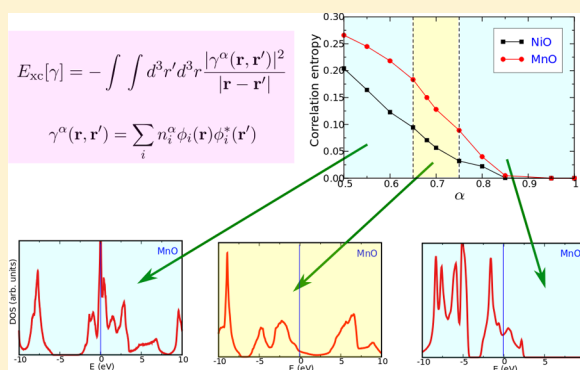
<sup>†</sup>Max-Planck-Institut für Mikrostrukturphysik, Weinberg 2, D-06120 Halle, Saxony-Anhalt, Germany

<sup>‡</sup>Department of Physics, Indian Institute of Technology, Roorkee, 247667 Uttarkhand, India

<sup>¶</sup>Lehrstuhl für Theoretische Festkörperphysik, Staudstrasse 7-B2, 91058 Erlangen, Bavaria, Germany

<sup>§</sup>Theoretical and Physical Chemistry Institute, National Hellenic Research Foundation, Vass. Constantinou 48, GR-11635 Athens, Greece

**ABSTRACT:** We demonstrate that reduced density matrix functional theory (RDMFT), in conjunction with the power functional, can successfully treat the nonmagnetic insulating state of the transition metal oxides NiO and MnO, finding for both a gapped single particle spectrum. While long-range spin order is thus not necessary for qualitative agreement with experiment, we find that it is required for good agreement with the X-ray photoemission spectroscopy and Bremsstrahlung isochromat spectroscopy data. We further examine the nature of the natural orbitals in the materials, finding that they display significant Hubbard localization and are, as a consequence, very far from the corresponding Kohn–Sham orbitals. This contrasts with the case of the band insulator Si, in which the Kohn–Sham orbitals are found to be very close to the RDMFT natural orbitals.



## 1. INTRODUCTION

A fully first-principles theory capable of treating strongly correlated solids remains the outstanding challenge of modern day materials science. This is exemplified by the failure of ground-state density function theory (DFT) to capture, in the absence of long-range magnetic order, the insulating state of the transition metals oxides (TMOs). This failure is particularly acute from the point of view of spectral information derived from DFT. Despite the absence of a rigorous theoretical link to the true single particle excitations of an interacting system, the Kohn–Sham (KS) eigenvalues are frequently of great practical utility and in many cases agree well with the X-ray photoemission spectroscopy (XPS) and Bremsstrahlung isochromat spectroscopy (BIS) experiments.<sup>1–4</sup> However, as the KS eigenvalues are derived from a noninteracting auxiliary system, for the TMOs such as MnO with an odd number of electrons per unit-cell it is *in principle impossible* for the KS spectrum to yield a gap for this material in the nonmagnetic state. The imposition of long-range magnetic order alleviates the problem to some extent; however, as the TMOs remain in experiment insulating in nature well above the Néel temperature, magnetic order is merely a co-occurring phenomena and cannot be the driving mechanism of the insulating state. In fact, not only ground-state DFT but also modern many-body techniques such as the *GW* method fail to capture the insulating behavior in TMOs without explicit long-range spin ordering.<sup>5–7</sup>

In this regard, the two many-body techniques that are able to capture the correct physics of strong correlations are dynamical mean field theory (DMFT)<sup>8–10</sup> and reduced density matrix functional theory (RDMFT);<sup>11</sup> these two methods predicts TMOs as insulators, even in the absence of long-range spin-order. This clearly points toward the ability of these techniques to capture physics well beyond the reach of most modern day ground-state methods.

Despite this success the effectiveness of RDMFT as a ground-state theory has been seriously hampered due to the absence of a technique for the determination of the spectral information. Recently, this final hurdle has also been removed, and the spectral information thus obtained for TMOs was shown to be in good agreement with experiments.<sup>12</sup> However, these spectra were calculated in the presence of antiferromagnetic order. The question then arises as to how effective RDMFT is in describing the insulating state of Mott insulators in the absence of long-range spin order. In order to answer this question, in the present work, we study the spectral properties of nonmagnetic NiO and MnO. Here the former is insulating due to the interplay of Mott localization and charge transfer effects, while the latter is insulating purely due to strong Mott localization. A detailed analysis of RDMFT and KS orbitals is performed which shows that, unlike in the case of band insulators, for Mott insulators the nature of two sets of orbitals

Received: July 10, 2015

Published: September 11, 2015

are very different, and this difference is indeed crucial for the success of RDMFT in describing Mott physics.

## 2. THEORY

Within RDMFT the one-body reduced density matrix (1-RDM) is the basic variable<sup>13,14</sup>

$$\gamma(\mathbf{r}, \mathbf{r}') = N \int d\mathbf{r}_2 \dots d\mathbf{r}_N \Phi^*(\mathbf{r}', \mathbf{r}_2 \dots \mathbf{r}_N) \Phi(\mathbf{r}, \mathbf{r}_2 \dots \mathbf{r}_N) \quad (1)$$

where  $\Phi$  denotes the many-body wave function. Diagonalization of this matrix produces a set of natural orbitals,<sup>15</sup>  $\phi_{jk}$  and occupation numbers,  $n_{jk}$  leading to the spectral representation

$$\gamma(\mathbf{r}, \mathbf{r}') = \sum_{j,k} n_{jk} \phi_{jk}(\mathbf{r}) \phi_{jk}^*(\mathbf{r}') \quad (2)$$

where the necessary and sufficient conditions for ensemble  $N$ -representability<sup>15</sup> of  $\gamma$  require  $0 \leq n_{jk} \leq 1$  for all  $j,k$ , and  $2 \sum_{j,k} n_{jk} = N$ . Here  $j$  represents the band index, and  $k$  represents the crystal momentum.

In terms of  $\gamma$ , the total ground-state energy<sup>14</sup> of the interacting system is (atomic units are used throughout)

$$E[\gamma] = -\frac{1}{2} \int \lim_{\mathbf{r} \rightarrow \mathbf{r}'} \nabla_{\mathbf{r}}^2 \gamma(\mathbf{r}, \mathbf{r}') d^3 r' + \int \rho(\mathbf{r}) V_{\text{ext}}(\mathbf{r}) d^3 r + \frac{1}{2} \int \frac{\rho(\mathbf{r}) \rho(\mathbf{r}')}{|\mathbf{r} - \mathbf{r}'|} d^3 r d^3 r' + E_{\text{xc}}[\gamma] \quad (3)$$

where  $\rho(\mathbf{r}) = \gamma(\mathbf{r}, \mathbf{r})$ ,  $V_{\text{ext}}$  is a given external potential, and  $E_{\text{xc}}$  we call the xc energy functional. In principle, Gilbert's<sup>14</sup> generalization of the Hohenberg–Kohn theorem to the 1-RDM guarantees the existence of a functional  $E[\gamma]$  whose minimum yields the exact  $\gamma$  and the exact ground-state energy of systems characterized by the external potential  $V_{\text{ext}}(\mathbf{r})$ . In practice, however, the correlation energy is an unknown functional of the 1-RDM and must be approximated. Although there are several known approximations for the xc energy functional,<sup>16–31</sup> the most promising for extended systems is the power functional<sup>11,12</sup> where the xc energy reads

$$E_{\text{xc}}[\gamma] = E_{\text{xc}}[\{\phi_{jk}\}, \{n_{jk}\}] = - \int \int d^3 r' d^3 r \frac{|\gamma^\alpha(\mathbf{r}, \mathbf{r}')|^2}{|\mathbf{r} - \mathbf{r}'|} \quad (4)$$

here  $\gamma^\alpha$  indicates the power used in the operator sense i.e.

$$\gamma^\alpha(\mathbf{r}, \mathbf{r}') = \sum_i n_i^\alpha \phi_i(\mathbf{r}) \phi_i^*(\mathbf{r}') \quad (5)$$

for  $\alpha = 1/2$  this is the Müller functional,<sup>32</sup> which is known to severely overestimate electron correlation<sup>33–36</sup> while for  $\alpha = 1$  this functional is equivalent to the Hartree–Fock method, which includes no correlations. If  $\alpha$  is chosen to be  $1/2 < \alpha < 1$ , the power functional interpolates between the uncorrelated Hartree–Fock limit and the overcorrelating Müller functional.

All calculations are performed using the full-potential linearized augmented plane wave code Elk,<sup>37</sup> with practical details of the calculations following the schemes described in refs 11 and 12. The calculations are performed using a shifted grid (by 0.01 0.01 0.03) of 125  $k$ -points in the irreducible Brillouin zone and a total of 2750 natural orbitals. A small smearing width of 27 meV was used for all calculations.

## 3. RESULTS

Presented in Figure 1 are the spectra for the Mott insulators under consideration. It is immediately apparent that RDMFT

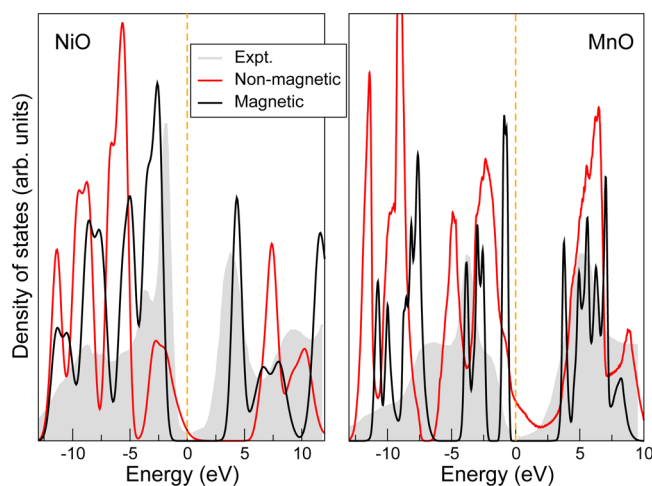


**Figure 1.** Density of states as a function of energy (in eV) for NiO (left panel) and MnO (right panel). Results are obtained with (black) and without (red) long-range (antiferromagnetic) spin order and with a value of  $\alpha = 0.68$ . For comparison experimental data taken from refs 2 and 4 is also shown (gray shaded area). Chemical potential is shown with a dotted vertical line.

captures the essence of Mott–Hubbard physics: both NiO and MnO present substantial gaps at the Fermi energy and are thus insulating in the absence of spin order. This fact was already noticed in a previous work<sup>11</sup> in which the presence of gap without any spin-order was deduced via very different techniques, namely the discontinuity in the chemical potential as a function of the particle number. A comparison of the nonmagnetic spectra with the experimental data shows that the shape of the conduction band is well reproduced for NiO. For MnO the position and width of the conduction band are well reproduced. Several peaks rather than one broad feature is present in RDMFT results due to the use of a very small smearing width (27 meV). The shape of the valence band is not in very good agreement with experiments for both NiO and MnO. This agreement improves on inclusion of the spin order, indicating that even though the insulating nature of TMO's is not driven by spin order, spin polarization significantly effects the spectra of these materials. This is hardly surprising given that NiO and MnO have very large local moments of  $1.9 \mu_B$  and  $4.7 \mu_B$ , respectively.

Correct treatment of correlations is crucial for TMOs, the prototypical strongly correlated materials. As mentioned above the power functional interpolates between two limits—the highly over correlated Müller ( $\alpha = 0.5$ ) and totally uncorrelated Hartree–Fock ( $\alpha = 1$ ). We now look at the effect of correlations, by varying  $\alpha$ , on the spectra of Mott insulators (NiO and MnO) and band insulator (Si), see Figure 2. The behavior of the spectra as a function of  $\alpha$  is rather trivial for the band insulator, Si; the valence bands rigidly shift lower in energy leading to increase in the band gap. The behavior for Mott insulators is different in that the shape of the bands change as a function of  $\alpha$ . Both for NiO and MnO over correlated Müller functional incorrectly gives a metallic ground-state. This leads to highly non-trivial behaviour as a function of  $\alpha$ , which must lie within a small range (between 0.65 and 0.7) in which the correct insulating ground-state is obtained. Reassuringly, the range of  $\alpha$  in which correct ground state behaviour is similar for both NiO and MnO. It is worth noting

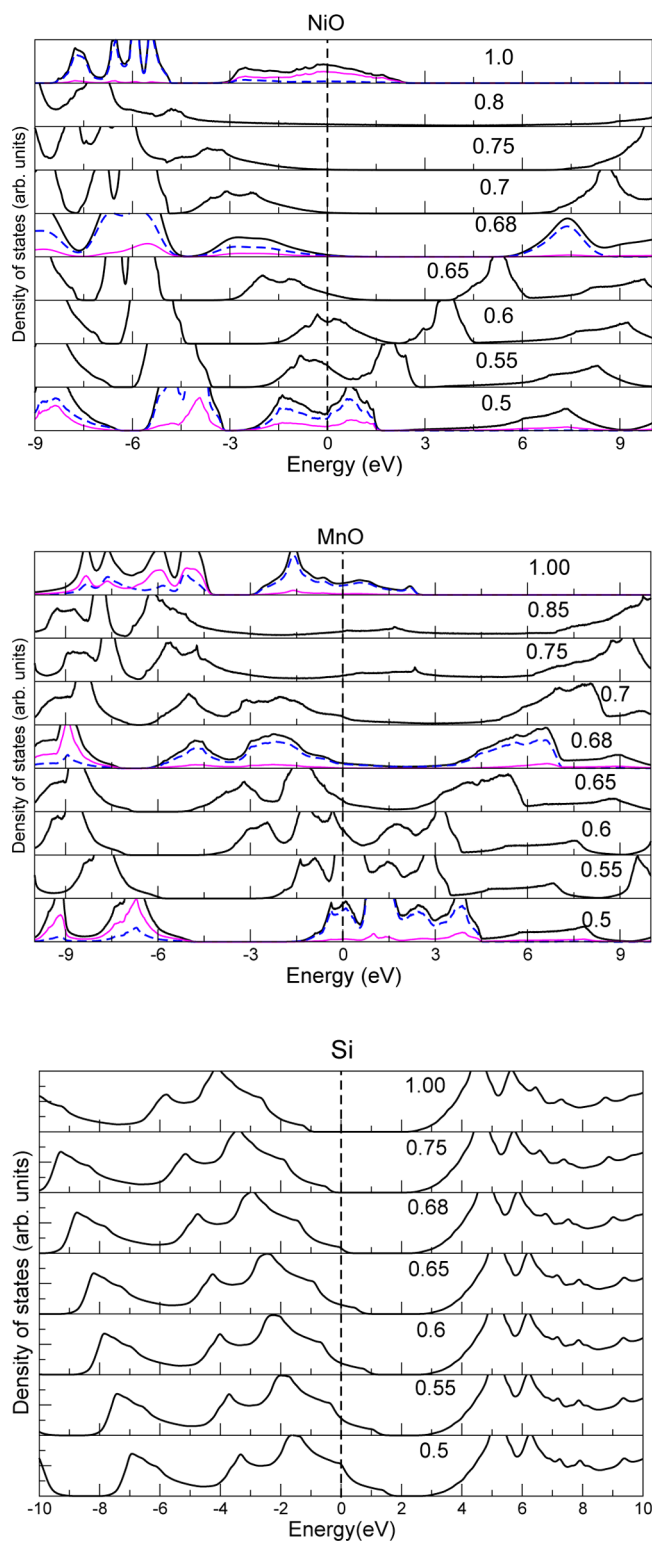


**Figure 2.** Density of states (DOS) as a function of energy (in eV) for NiO (upper panels), MnO (middle panels), and Si (lower panels). The transition metal-*d* (dotted blue line) and O-*p* (thin pink line) projected DOS are also presented for NiO and MnO. The results are obtained using different values of  $\alpha$  in eq 4. Chemical potential is shown with a dotted vertical line.

that the RDMFT also gives the correct symmetry of the gap (i.e. between transition metal-*d* states).

To understand this interesting behavior it is instructive to look at the correlation entropy,<sup>38</sup>  $S$ , as a function of  $\alpha$

$$S = \frac{-\sum_i n_i \ln(n_i)}{\sum_i n_i} \quad (6)$$

$S$  can be regarded as measure of correlations, being maximum for highly correlated systems and 0 in the totally uncorrelated case. Correlation entropy as a function of  $\alpha$  is plotted for NiO and MnO in Figure 3. Hartree–Fock, being a single particle

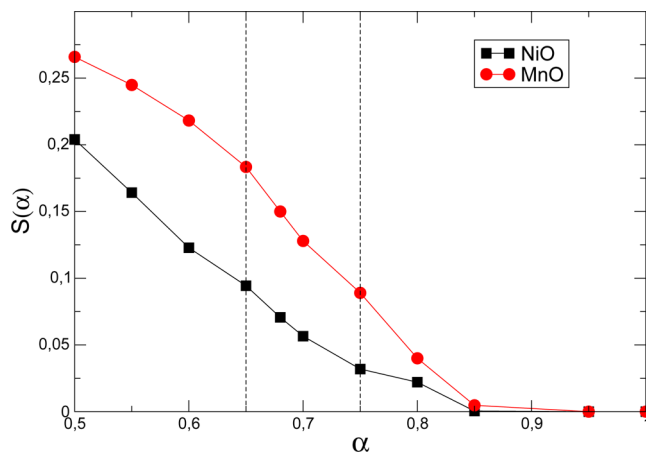


**Figure 3.**  $S$  (eq 6) as a function of  $\alpha$  for NiO (black squares) and MnO (red circles). The optimal value of  $\alpha$  lies between 0.65 and 0.7, and this region is indicated by dotted vertical lines.

theory, leads to pinned occupation numbers (i.e.,  $n_i = 1$  or  $n_i = 0$ ) and hence  $S = 0$ . For RDMFT with  $\alpha > 0.8$  similar behavior is observed (i.e., most of the occupation numbers are pinned) leading again to almost uncorrelated results. It is interesting to note that small values of  $\alpha$ , which lead to over correlation, also results in a metallic ground state. That over correlation<sup>39,40</sup> leads to incorrect ground state which is well-known from previous studies.<sup>36,39</sup> Present results further highlight the importance of the right amount of correlation required to get the correct ground state of the material. From Figure 3 we can also infer that, within RDMFT, MnO is more strongly correlated than NiO, which has already been noted before in the literature.<sup>8,9,41</sup>

Within RDMFT there are no Kohn–Sham-like equations to solve, and a direct minimization over natural orbitals and occupation numbers is required while maintaining the ensemble  $N$ -representability conditions. The minimization over occupation numbers is computationally very efficient (for details see ref 11), but the same cannot be said about the minimization over the natural orbitals. In practical terms, the natural orbitals (see eq 2) are expanded in a set of previously converged KS states, and optimization of the natural orbitals is performed by varying the expansion coefficients. This procedure allows us to examine how different KS states are from fully optimized natural orbitals. In the present work these KS states were obtained using local density approximation (LDA).<sup>42</sup>

In Figure 4 three set of results are shown: (i) KS density of states, (ii) RDMFT density of states obtained without optimizing the natural orbitals i.e. by using KS orbitals as natural orbitals but fully optimizing the occupation numbers, and (iii) the fully optimized RDMFT results i.e. full

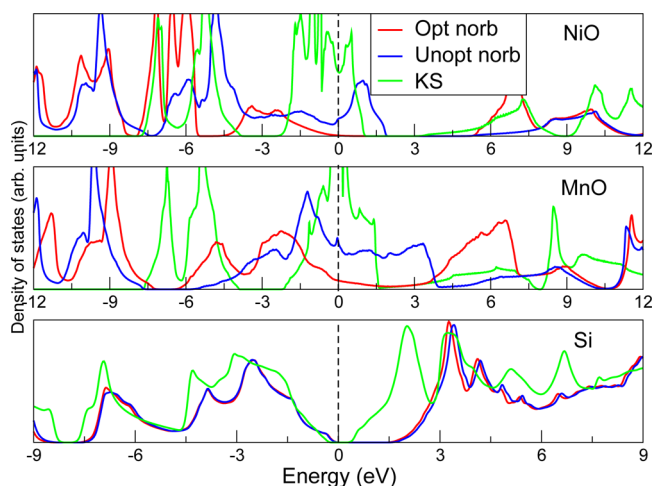


**Figure 4.** Density of states as a function of energy (in eV) for NiO (top panel), MnO (middle panel), and Si (lower panel). Results are obtained with (red) and without (blue) optimization of the natural orbitals within RDMFT. KS results (green) are obtained using local density approximation.<sup>42</sup> Chemical potential is shown with a dotted vertical line.

optimization over the natural orbitals and occupation numbers. From these results it is clear that for the band insulator Si it is sufficient to optimize the occupation numbers to increase the band gap in line with experiment; the KS states are evidently already a very good representation of the natural orbitals. As may be seen in Figure 4 the opposite situation holds for the case of the Mott insulators NiO and MnO: clearly the KS states differ profoundly from the natural orbitals. In this case it is crucial to optimize the natural orbitals. The reason for this is that in the case of Mott insulators it is the localization of electrons which leads to formation of the gap and KS orbitals are not sufficiently localized, thus optimization over the natural orbitals is required.

A confirmation of this charge localization may be seen in the charge density. In Figure 5 we plot the difference  $\rho(\mathbf{r}) - \rho_{LDA}(\mathbf{r})$ , for (i) RDMFT (lower panel) and (ii) the LSDA+*U* functional<sup>43</sup> (upper panel) within DFT for NiO. The LSDA+*U* method is chosen because, like RDMFT, it also finds the correct insulating ground state for NiO.<sup>5,44</sup> However, the LSDA+*U* method achieves this by both spin order and on-site Hubbard *U* and, in contrast to RDMFT, cannot treat the nonmagnetic insulating state of this material. The impact of this on the charge density is clear in Figure 5: significant charge localization is seen only in the RDMFT density. Interestingly, one observes an almost spherical charge accumulation at the oxygen site, a result in agreement with experiment<sup>45</sup> but different from that found in the corresponding LSDA+*U* result.

#### 4. SUMMARY

To summarize, in this work we demonstrate that RDMFT in conjunction with the power functional is able to capture the insulating state of NiO and MnO in the absence of long-range spin order. However, while spin order does not drive the insulating ground state, the large local moments in these materials require spin be explicitly taken into account for excellent agreement with experimental spectra to be obtained. The power,  $\alpha$ , in the power functional is an indicator of the amount of correlation, and a detailed analysis shows a highly nontrivial behavior of the spectra for Mott insulators as a

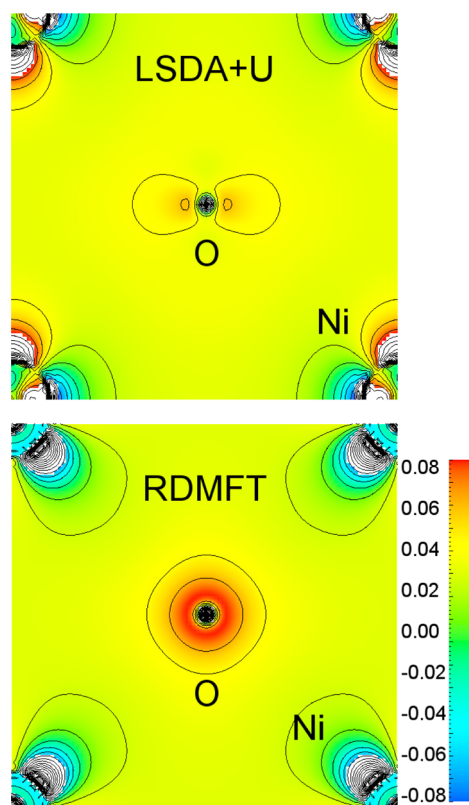


**Figure 5.** Difference between the LSDA charge density and charge density calculated using LSDA+*U* and RDMFT,  $(\rho(\mathbf{r}) - \rho_{LSDA}(\mathbf{r}))$  for NiO. Positive values indicate localization of charge as compared to LSDA.

function of  $\alpha$ , which must lie within a small range (between 0.65 and 0.7) for the correct insulating ground state to be obtained.

We have also examined the nature of the natural orbitals in these materials, as well as in classic band insulator Si. For Si the Kohn–Sham orbitals provide a very good approximation to the RDMFT natural orbitals, and minimization over the RDMFT occupation numbers alone already yields spectral information in very good agreement with experiments. This is not the case for NiO and MnO as strong Hubbard correlation drives a significant charge localization, absent in the corresponding DFT calculation, which renders the KS orbitals significantly different from the RDMFT natural orbitals. This serves to highlight the fundamental difference in the way that a many-body theory such as RDMFT treats strong correlation, as compared to DFT based band theory methods such as LSDA+*U*. While the latter theory is capable of capturing the ground-state spectrum, the LSDA+*U* orbitals are not sufficiently localized. For the case of NiO a consequence of this is that while the RDMFT density shows a significant charge accumulation at the oxygen site in agreement with experiment, this is absent in the LSDA+*U* charge density.

#### ■ AUTHOR INFORMATION

##### Corresponding Author

\*E-mail: sharma@mpi-halle.mpg.de.

##### Notes

The authors declare no competing financial interest.

## ■ ACKNOWLEDGMENTS

N.N.L. acknowledges support by the GSRT, Greece, POLYNANO-KRIPIS project (447963). S.S. would like to acknowledge Stefano di Sabatino and Pina Romaniello for discovering a convergence issue with the Hartree–Fock results.

## ■ REFERENCES

- (1) Ulmer, K. *Phys. Rev. Lett.* **1959**, *3*, 514.
- (2) van Elp, J.; Potze, R. H.; Eskes, H.; Berger, R.; Sawatzky, G. A. *Phys. Rev. B: Condens. Matter Mater. Phys.* **1991**, *44*, 1530.
- (3) van Elp, J.; Wieland, J. L.; Eskes, H.; Kuiper, P.; Sawatzky, G. A.; de Groot, F. M. F.; Turner, T. S. *Phys. Rev. B: Condens. Matter Mater. Phys.* **1991**, *44*, 6090.
- (4) Sawatzky, G. A.; Allen, J. W. *Phys. Rev. Lett.* **1984**, *53*, 2339.
- (5) Rödl, C.; Fuchs, F.; Furthmüller, J.; Bechstedt, F. *Phys. Rev. B: Condens. Matter Mater. Phys.* **2009**, *79*, 235114.
- (6) Aryasetiawan, F.; Gunnarsson, O. *Phys. Rev. Lett.* **1995**, *74*, 3221.
- (7) Kobayashi, S.; Ohara, Y.; Yamamoto, S.; Fujiwara, T. *Phys. Rev. B: Condens. Matter Mater. Phys.* **2008**, *78*, 155112.
- (8) Ren, X.; Leonov, I.; Keller, G.; Kollar, M.; Nekrasov, I.; Vollhardt, D. *Phys. Rev. B: Condens. Matter Mater. Phys.* **2006**, *74*, 195114.
- (9) Kunes, J.; Lukoyanov, A. V.; Anisimov, V. I.; Scalettar, R. T.; Pickett, W. E. *Nat. Mater.* **2008**, *7*, 198.
- (10) Miura, O.; Fujiwara, T. *Phys. Rev. B: Condens. Matter Mater. Phys.* **2008**, *77*, 195124.
- (11) Sharma, S.; Dewhurst, J. K.; Lathiotakis, N. N.; Gross, E. K. U. *Phys. Rev. B: Condens. Matter Mater. Phys.* **2008**, *78*, 201103.
- (12) Sharma, S.; Dewhurst, J. K.; Shallicross, S.; Gross, E. K. U. *Phys. Rev. Lett.* **2013**, *110*, 116403.
- (13) Lödwig, P. O. *Phys. Rev.* **1955**, *97*, 1974.
- (14) Gilbert, T. L. *Phys. Rev. B* **1975**, *12*, 2111.
- (15) Coleman, A. *Rev. Mod. Phys.* **1963**, *35*, 668.
- (16) Müller, A. M. K. *Phys. Rev. A* **1984**, *105*, 446.
- (17) Gritsenko, O.; Pernal, K.; Baerends, E. J. *J. Chem. Phys.* **2005**, *122*, 204102.
- (18) Rohr, D. R.; Toulouse, J.; Pernal, K. *Phys. Rev. A: At, Mol., Opt. Phys.* **2010**, *82*, 052502.
- (19) Rohr, D. R.; Pernal, K.; Gritsenko, O. V.; Baerends, E. J. *J. Chem. Phys.* **2008**, *129*, 164105.
- (20) Marques, M. A. L.; Lathiotakis, N. N. *Phys. Rev. A: At, Mol., Opt. Phys.* **2008**, *77*, 032509.
- (21) Piris, M. *Int. J. Quantum Chem.* **2006**, *106*, 1093.
- (22) Giesbertz, K. J. H.; Gritsenko, O. V.; Baerends, E. J. *Phys. Rev. Lett.* **2010**, *105*, 013002.
- (23) Piris, M.; Lopez, X.; Ruipérez, F.; Matxain, J. M.; Ugalde, J. M. *J. Chem. Phys.* **2011**, *134*, 164102.
- (24) Pernal, K. *J. Chem. Theory Comput.* **2014**, *10*, 4332.
- (25) Lathiotakis, N. N.; Helbig, N.; Rubio, A.; Gidopoulos, N. I. *Phys. Rev. A: At, Mol., Opt. Phys.* **2014**, *90*, 032511.
- (26) Piris, M.; Matxain, J. M.; Lopez, X. *J. Chem. Phys.* **2013**, *139*, 234109.
- (27) Giesbertz, K. J. H.; Pernal, K.; Gritsenko, O. V.; Baerends, E. J. *J. Chem. Phys.* **2009**, *130*, 114104.
- (28) Piris, M.; Matxain, J. M.; Lopez, X.; Ugalde, J. M. *J. Chem. Phys.* **2012**, *136*, 174116.
- (29) Chatterjee, K.; Pernal, K. *J. Chem. Phys.* **2012**, *137*, 204109.
- (30) van Meer, R.; Gritsenko, O. V.; Giesbertz, K. J. H.; Baerends, E. J. *J. Chem. Phys.* **2013**, *138*, 094114.
- (31) Lathiotakis, N. N.; Helbig, N.; Rubio, A.; Gidopoulos, N. I. *J. Chem. Phys.* **2014**, *141*, 164120.
- (32) Müller, A. M. K. *Phys. Lett. A* **1984**, *105*, 446.
- (33) Csányi, G.; Arias, T. A. *Phys. Rev. B: Condens. Matter Mater. Phys.* **2000**, *61*, 7348.
- (34) Gritsenko, O.; Pernal, K.; Baerends, E. J. *J. Chem. Phys.* **2005**, *122*, 204102.
- (35) Herbert, J. M.; Harriman, J. E. *Chem. Phys. Lett.* **2003**, *382*, 142.
- (36) Lathiotakis, N. N.; Helbig, N.; Gross, E. K. U. *Phys. Rev. B: Condens. Matter Mater. Phys.* **2007**, *75*, 195120.
- (37) (2004), URL <http://elk.sourceforge.net> (accessed Sept 1, 2015).
- (38) Ziesche, P. *Int. J. Quantum Chem.* **1995**, *56*, 363.
- (39) Lathiotakis, N.; Sharma, S.; Dewhurst, J.; Eich, F.; Marques, M.; Gross, E. *Phys. Rev. A: At, Mol., Opt. Phys.* **2009**, *79*, 040501.
- (40) Lathiotakis, N. N. *Int. J. Quantum Chem.* **2013**, *113*, 762.
- (41) Kunes, J.; anisimov, V. I.; Lukoyanov, A. V.; Vollhardt, D. *Phys. Rev. B: Condens. Matter Mater. Phys.* **2007**, *75*, 165115.
- (42) Perdew, J. P.; Wang, Y. *Phys. Rev. B: Condens. Matter Mater. Phys.* **1992**, *45*, 13244.
- (43) Liechtenstein, A. I.; Anisimov, V. I.; Zaanen, J. *Phys. Rev. B: Condens. Matter Mater. Phys.* **1995**, *52*, R5467.
- (44) Shinohara, Y.; Sharma, S.; Dewhurst, J. K.; Shallicross, S.; Lathiotakis, N. N.; Gross, E. K. U. URL <http://arxiv.org/abs/1206.1713> (accessed Sept 1, 2015).
- (45) Dudarev, S. L.; Peng, L.-M.; Savrasov, S. Y.; Zuo, J.-M. *Phys. Rev. B: Condens. Matter Mater. Phys.* **2000**, *61*, 2506.